In situ laser crystallization of amorphous silicon: Controlled nanosecond studies in the dynamic transmission electron microscope

M. L. Taheri,[1,a)] S. McGowan,[2] L. Nikolova,[3] J. E. Evans,[4,5] N. Teslich,[4] J. P. Lu,[6] T. LaGrange,[4] F. Rosei,[3] B. J. Siwick,[2] and N. D. Browning[4,5,7]
[1]*Department of Materials Science and Engineering, Drexel University, Philadelphia, Pennsylvania 19104, USA*
[2]*Departments of Physics and Chemistry, Center for the Physics of Materials, McGill University, Montreal H3A2T8, Canada*
[3]*Institut National de la Recherche Scientifique, Energie, Materiaux et Telecommunications, Varennes, Québec J3X1S2, Canada*
[4]*Physical and Life Sciences Directorate, Lawrence Livermore National Laboratory, Livermore, California 94550, USA*
[5]*Department of Molecular and Cellular Biology, University of California-Davis, Davis, California 95616, USA*
[6]*Palo Alto Research Center (PARC), Palo Alto, California 94394, USA*
[7]*Department of Chemical Engineering and Materials Science, University of California-Davis, Davis, California 95616, USA*

(Received 6 March 2009; accepted 13 April 2010; published online 19 July 2010)

We describe an *in situ* method for studying the influence of deposited laser energy on microstructural evolution during nanosecond laser driven crystallization of amorphous Si. By monitoring microstructural evolution as a function of deposited energy in a dynamic transmission electron microscope (DTEM), information on grain size and defect concentration can be correlated directly with processing conditions. This work demonstrates that DTEM studies are a promising approach for obtaining fundamental information on nucleation and growth processes that have technological importance for the development of thin film transistors. © *2010 American Institute of Physics*. [doi:10.1063/1.3422473]

Polycrystalline silicon (poly-Si) is of technological interest for use in thin film transistors (TFT) applications.[1,2] Understanding the role of grain size and defect concentration holds the promise to control poly-Si properties. Industrial processing of poly-Si films proceeds through crystallization of amorphous silicon (a-Si) using laser irradiation such as escimer lasers.[1] While the role of grain size and defects on device performance has been investigated *ex situ*, an approch that allows microstructure formation to be studied *during* processing would represent a breakthrough. As crystallization phase front velocities for this type of experiment were previously found to be 10 m/s,[2]such observations require high temporal resolution. Here we present a method for studying pulse laser induced crystallization of (a-Si) films with a temporal resolution of ~10 ns using the dynamic transition electron microscope (DTEM). The DTEM has been used previously for *ex situ* TEM experiments[3–7] and laser processing materials.[7,8] We show here that a-Si films can be crystallized using *ex situ* pulses laser heating and the crystallization process can be tracked using high time resolution.

The DTEM consists of a JEOL 2000FX TEM column modified to provide access for the two pulsed lasers: the "drive laser" and the "cathode laser". The drive laser is used to initiate a transient state in the sample such as a phase change or reaction, while the photocathode laser generates the pulsed electron beam used for imaging. The relative timing of these two laser pulses is set electronically and determines the time delay at which the TEM image is acquired after the drive laser interacts with specimen. This instrument is described in detail elsewhere.[6]

One advantage of the DTEM instrument design is that it can operate in either pulsed photoemission mode or in a conventional thermionic continuous wave (CW) mode. The pulsed mode's ns-scale imaging capability greatly exceeds the ~30 Hz time resolution of conventional *in situ* TEM. In this letter, we first present results of *in situ* observation of the laser-induced phase transition using the conventional CW imaging. Next, we present results obtained by taking advantage of the DTEM's capabilities to study the microstructural evolution on ns time scales. Although *in situ* analysis of melting and solidification of thin films as a function of incident laser energy has been studied, e.g., by flash laser photography,[9,10] these techniques give little information about microstructural evolution.

Wafers of 50 nm a-Si/700 nm SiO_2/glass were provided by Palo Alto Research Center (PARC), and electron transparent films were prepared using a FEI Nova600 Focused Ion Beam (FIB). First, the sample was ground to a thickness of ~20 μm. Then, the FIB was used to prepare films by preferential thinning of the SiO_2 side. Initial thinning was performed at 30 kV and 20 nA to a thickness of ~2 μm, then subject to further thinning at progressivley lower beam currents, from 0.3 nA to 0.1 nA, producting 50 nm a-Si/SiO_2 films (Fig. 1). In addition, 110 nm thick a-Si films (used for data presented in Fig. 3) were deposited by electron beam evaporation onto TEM grids containing nine 100 $\times$ 100 μm^2 windows.

In our first experiments, films were processed *in situ* in

a)Author to whom correspondence should be addressed. Electronic mail: mtaheri@coe.drexel.edu.

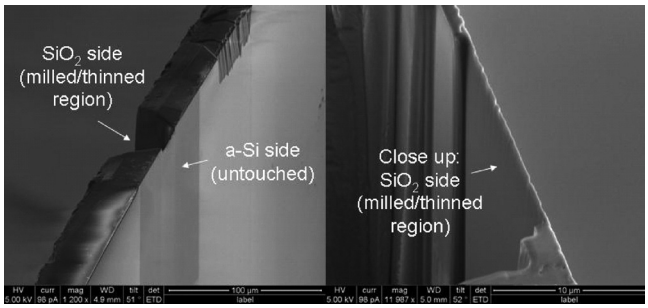

FIG. 1. Secondary electron beam images showing FIB-thinned samples. The flat, untouched region shown on the left is the a-Si surface. The back-thinning process is shown on the right. Films of a width of greater than approximately 100 by 100 microns were prepared. The origin of the stripes in the image is the ion beam raster.

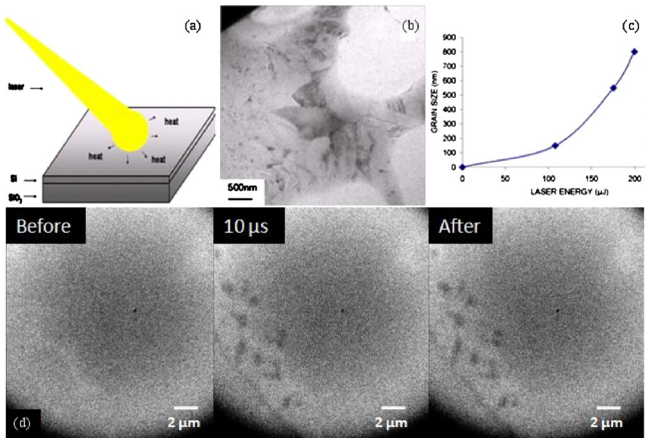

FIG. 2. (Color online) Schematic of drive laser incident on sample (a) cw electron beam images showing plan views of film shot at ~108 and 175.5 μJ (b) Maximum grain size after crystallization experiment as a function of laser energy. (c) Grain size=approximate diameter of largest grain shown in field of view; and sequence of images of microstructure at 10 μs time delay for a fluence of ~108 μJ (d).

the DTEM using 355 nm light [Fig. 2(a)] while the grain growth and morphology were observed after melt-mediated solidification. Figure 2(b) shows cw image after irradiating the sample with ~175.5 μJ, in a 50 μm diameter spot. The absence of material in the center spot suggests that the silicon dewets from the substrate, and super lateral growth (SLG) is seen in the rectangular shaped grains. The rapid lateral solidification starts at the periphery of laser spot and anisotropic (or nonequiaxed) grains nucleate at the melted/nonmelted interface and grow inward parallel to the direction of solidification. This morphology mimics similar microstructural features previously reported by Moon *et al.*, where directional solidification resulted from interfacial under-cooling.[13] In studies by Im *et al.*,[11,14] a small but gradual increase in grain size with laser fluence in the low energy (partial-melting) regime was observed. They noted that in a "near-complete" melting regime a substantially enlarged grain size was obtained; the grain size increases with fluence until 25 mJ cm^{-2} (above the full melt threshold),

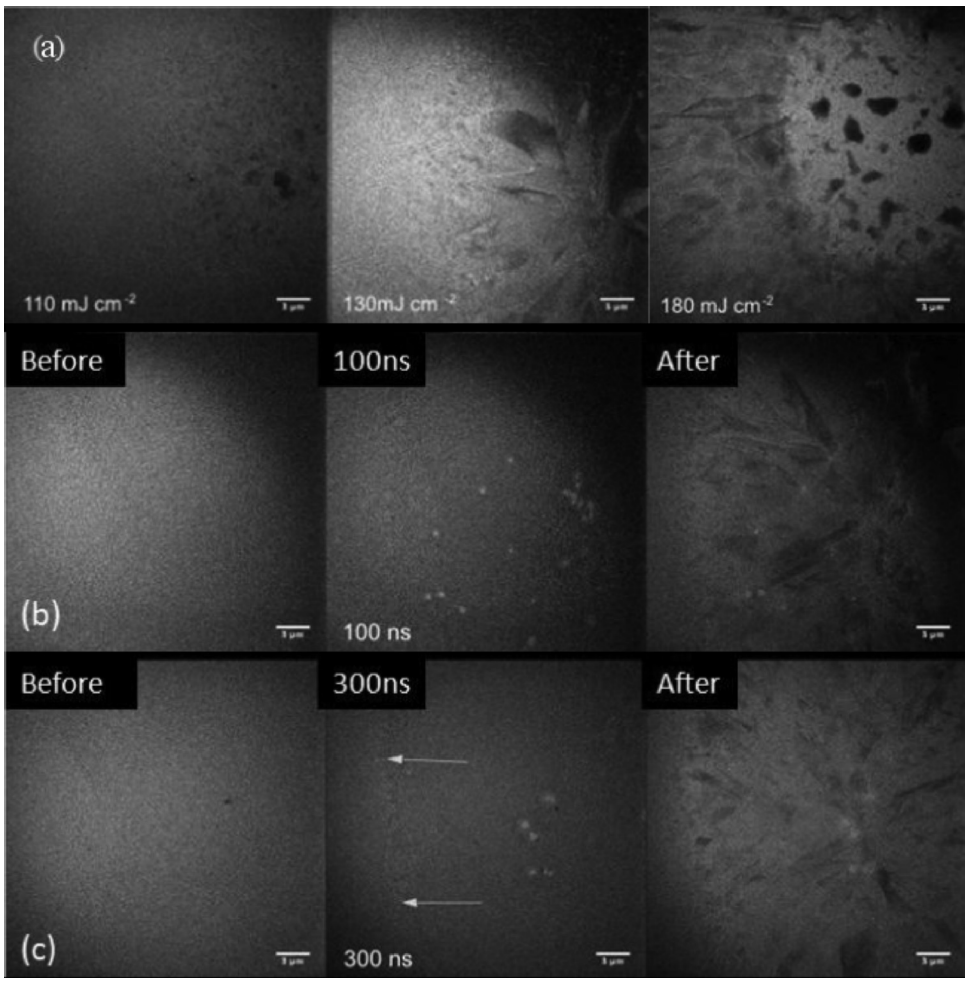

FIG. 3. Sequence of images of microstructure as function of the incident laser fluence (a) sequence of images for fluence of 155 mJ/cm^2 at 100 ns and 300 ns time delays [(b) and (c)], respectively.

beyond which material crystallized into a fine-grained microstructure. In Fig. 2(c), we also observe a nonlinear increase in grain size with energy. In contrast to the Im *et al.* experiments at high fluences above the melt threshold, the molten Si dewets from the SiO_2 substrate and coalelscles into droplets that solidify into large grains. Despite the presence of lateral solidification in localized regions of melting, our results suggest that the thin layer specimen geometry inhibited heat flow, yielding slow lateral grain growth at high laser fluences (instead of an adequate heat sink leading to fine grain size), and cannot be directly compared to large-scale experiments.[11–14]

Figure 2(d) shows a series of pulsed electron DTEM bright field images of the material taken before laser irradiation at 355 nm, 10 μs after the drive laser pump pulse, and after the material cooled to room temperature. Although the quality of the images from these early DTEM experiments are not up to the level of more recent results (see Fig. 3), the relevant features are visible and these experiments indicate that crystallization and subsequent microstructural evolution occur on time scales less than 10 μs.

Further experiments on shorter time scales were conducted in the upgraded DTEM providing higher pulsed electron currents, thus improving the image detail of the crystallization process. In addition, crystallization was induced using 532 nm laser light, since the thresholds for melt-mediated crystallization are comparable to 355 nm and the laser system has the advantage of lower shot to shot energy variation at 532 nm. In these experiments, we aimed to elucidate details of the partial and complete melt-mediated crystallization of the a-Si films on time scales less than 1 μs. Figure 3(a) shows the variation in postmortem microstructure as a function of fluence. The a-Si melts at fluences of $\sim$100 mJ cm^{-2}. The postmortem image on the left of Fig. 3(a) was irradiated to a fluence above this threshold and the large grains surrounded by fine-grained material on the right side of this image suggest that partial melting has occurred. Such microstructures are thought to occur by the SLG process in which the a-Si is melted and solidifies by rapid, anisotropic growth at the liquid-solid interface.[11] It is believed that in order to have such solidification mechanisms, solid state crystallization must first occur at the periphery of the molten Si pool or there must be nanocrystalline phases in the a-Si that act as nucleation sites for the rapid, lateral growth that produce these large grains. At higher fluences, more molten Si is produced and thus more material is crystallized via the SLG process, producing the large grains shown the center image of Fig. 3(a). However, dewetting of the molten Si from the SiO_2 occurs at fluences above 160 mJ cm^{-2} (see the right image in Fig. 3(a)), producing a discontinuous film with voids near the center of the laser spot.

Time resolved images (Figs. 3(b) and 3(c)) were taken at a fluence of 155 mJ cm^{-2}. The cooling rate in these samples is governed by the lateral heat diffusion and impacts the rates in which the SLG process occurs. Given a rough estimation of the cooling rate (10^8 K s^{-1}), several hundred nanoseconds are required to cool below the melt temperature and initiate solidification, as suggested by the emergence of the crystallization front on this timescale in the series in Figs. 3(b) and 3(c). At time delays of 100 ns, the material is still molten (note the voids in the center of the Figs. 3(b) and 3(c) which result for the substrate outgassing trapped residual gases at high temperature that form bubbles in the molten Si). After 300 ns, the fine grained material is visible at the edge of the laser irradiation zone and molten Si begins to solidify (denoted by the arrows in center image of Fig. 3(c)). The fine grained material is formed via solid-state crystallization, and the grains then act as nucleation sites for the rapid solidification.

In conclusion, we developed a method for studying laser processing of Si films *in situ* on ns time scales, which further elucidates microstructural evolution during various solidification regimes. Future studies will examine defect formation and grain size distribution with respect to the laser energy and adsorption depth in different substrates.

This work performed under the auspices of the U.S. Department of Energy by Lawrence Livermore National Laboratory and supported by the Office of Science, Office of Basic Energy Sciences, Division of Materials Sciences and Engineering, of the U.S. Department of Energy under Contract No. DE-AC52-07NA27344. The authors thank PARC for generous provision of wafers, and Rick Gross of LLNL for help with pre-FIB sample preparation. L.N. acknowledges a personal fellowship (CGS-D) from NSERC. F.R. and B.J.S. are grateful to the Canada Research Chairs program for partial salary support, and are funded by NSERC (Canada), FQRNT, and MDEIE (Quebec).

[1] S. Uchikoga and N. Ibaraki, Thin Solid Films **383**, 19 (2001).
[2] J. B. Boyce, P. Mei, R. T. Fulks, and J. Ho, Phys. Status Solidi A **166**, 729 (1998).
[3] T. LaGrange, M. R. Armstrong, K. Boyden, C. G. Brown, G. H. Campbell, J. Colvin, W. J. Dehope, A. M. Frank, D. J. Gibson, F. V. Hartemann, J. S. Kim, W. E. King, B. J. Pyke, B. W. Reed, M. D. Shirk, R. M. Shuttlesworth, B. C. Stuart, B. R. Torralva, and N. D. Browning, Appl. Phys. Lett. **89**, 044105 (2006).
[4] W. E. King, M. Armstrong, V. Malka, B. W. Reed, and A. Rousse, MRS Bull. **31**, 614 (2006).
[5] T. LaGrange, G. H. Campbell, P. E. A. Turchi, and W. E. King, Acta Mater. **55**, 5211 (2007).
[6] M. Armstrong, K. Boyden, N. D. Browning, G. H. Campbell, J. D. Colvin, W. DeHope, A. M. Frank, D. J. Gibson, F. Hartemann, J. S. Kim, W. E. King, T. B. LaGrange, B. J. Pyke, B. W. Reed, R. M. Shuttlesworth, B. C. Stuart, and B. R. Torralva, Ultramicroscopy **107**, 356 (2007).
[7] M. L. Taheri, T. B. Lagrange, B. W. Reed, M. R. Armstrong, G. H. Campbell, W. J. DeHope, J. S. Kim, W. E. King, D. J. Masiel, and N. D. Browning, Microsc. Res. Tech. **72**, 122 (2009).
[8] M. L. Taheri, T. Lagrange, B. W. Reed, and N. D. Browning, Small **12**, 2187 (2008).
[9] T. Y. Choi, D. J. Hwang, and C. P. Grigoropoulos, Opt. Eng. (Bellingham) **42**, 3383 (2003).
[10] M. Lee, S. Moon, and C. P. Grigoropoulos, J. Cryst. Growth **226**, 8 (2001).
[11] J. S. Im, H. J. Kim, and M. O. Thompson, Appl. Phys. Lett. **63**, 1969 (1993).
[12] R. S. Sposili and J. S. Im, Appl. Phys. Lett. **69**, 2864 (1996).
[13] S.-J. Moon, M. Lee, and C. P. Grigoropoulos, ASME J. Heat Transfer **124**, 253 (2002).
[14] M. Hatano, S. Moon, M. Lee, K. Suzuki, and C. P. Grigoropoulos, J. Appl. Phys. **87**, 36 (2000).